Radiation Physics and Chemistry 176 (2020) 108979

Contents lists available at ScienceDirect

Radiation Physics and Chemistry

journal homepage: www.elsevier.com/locate/radphyschem

Thermal disorder and anharmonicity of cesium iodide in EXAFS theory

Tran Thi Ha[a,b,*], Nguyen Ba Duc[c,**], Nguyen Van Nghia[d], Pham Thi Minh Hanh[e], Vu Thi Thanh Ha[h], Ho Khac Hieu[f,g,***]

[a] Laboratory of Advanced Materials Chemistry, Advanced Institute of Materials Science, Ton Duc Thang University, Ho Chi Minh City, 758307, Viet Nam
[b] Faculty of Applied Sciences, Ton Duc Thang University, Ho Chi Minh City, 758307, Viet Nam
[c] Tan Trao University, Km 6, Yen Son, Tuyen Quang, 301910, Viet Nam
[d] Faculty of Electrical and Electronics Engineering, Thuyloi University, 175 Tay Son, Dong Da, Ha Noi, 116705, Viet Nam
[e] Hanoi Pedagogical University No2, Nguyen Van Linh, Vinh Phuc, 15900, Viet Nam
[f] Institute of Research and Development, Duy Tan University, 03 Quang Trung, Hai Chau, Da Nang, 550000, Viet Nam
[g] Faculty of Natural Sciences, Duy Tan University, 03 Quang Trung, Hai Chau, Da Nang, 550000, Viet Nam
[h] Vietnam Education Publishing House, 234 Pham Van Dong, Ha Noi, 143330, Viet Nam

ARTICLE INFO

Keywords:
Anharmonicity
Thermal disorder
CsI
Debye model
EXAFS cumulants

ABSTRACT

In extended X-ray absorption fine structure (EXAFS) theory, the thermal disorder can be described by means of the moments of atomic displacement so-called EXAFS cumulants. In this work, thermal disorder and anharmonicity of cesium iodide (CsI) have been studied based on the anharmonic correlated Debye model in EXAFS theory. Analytical expressions of the first three EXAFS cumulants and the anharmonic factor were derived. Numerical calculations have been performed to determine these thermodynamic quantities of CsI up to temperature 700 K using the Lennard-Jones potential combined with Coulomb interaction contribution. It showed that the anharmonicity of thermal lattice vibrations gave significant contributions to the EXAFS cumulants. By investigation of the anharmonic factor in EXAFS theory we highlight the importance of anharmonicity not only at high temperature but also at low temperature in CsI crystal. This behavior of cesium iodide departs from copper metal, where the anharmonic contribution was unveiled almost zero at temperature below 100 K.

1. Introduction

Cesium halides (such as cesium chloride (CsCl), cesium bromide (CsBr), and cesium iodide (CsI)) with simple CsCl structure (B2, $Pm\bar{3}m$) exhibit many outstanding physical properties such as large dielectric constant (Bingol et al., 2015), and low lattice thermal conductivity (Gerlich and Andersson, 1982). These properties have been clarified closely related to phonon-phonon scattering as well as phonon anharmonicity (Sist et al., 2017; Wei et al., 2019). In condensed matter physics, anharmonicity in a system is mathematically described by a nonlinear relation between force and atomic displacement which departs from linear harmonic behavior. It was revealed to have a significant contribution to many fascinating physical properties including the negative thermal expansion (Li et al., 2011), high-T_c superconductivity (Bang et al., 2009), multiferroicity (Bansal et al., 2018) and lattice thermal conductivity (Li et al., 2015). Interestingly, whereas phonon anharmonicity is usually found at high temperatures because of the large amplitude of the atomic vibration, low temperature anharmonicity was discovered existing in cesium halides. For example, this unusual phenomenon was recently experimentally observed in CsI from inelastic neutron scattering measurements (Wei et al., 2019), and in CsCl by high-resolution X-ray diffraction (Sist et al., 2017).

The extended X-ray absorption fine structure (EXAFS) is a powerful method to investigate thermal behavior of materials (Willis and Pryor, 1975; Crozier et al., 1988; Hung et al., 2010). Previously, in the framework of the ab-initio EXAFS data-analysis (GNXAS method) combining with EXAFS measurements and reliable molecular dynamics simulations, the anharmonic effects in solid KBr (Cicco et al., 1996) and AgBr (Di Cicco et al., 2000) were investigated. The authors pointed out that the first-neighbor distribution functions of these two binary compounds are strongly asymmetric even at moderate temperature (Cicco et al., 1996; Di Cicco et al., 2000). Nevertheless, to our best knowledge,

* Corresponding author. Laboratory of Advanced Materials Chemistry, Advanced Institute of Materials Science, Ton Duc Thang University, Ho Chi Minh City, 758307, Viet Nam.
** Corresponding author.
*** Corresponding author. Institute of Research and Development, Duy Tan University, 03 Quang Trung, Hai Chau, Da Nang, 550000, Viet Nam.
E-mail addresses: tranthiha@tdtu.edu.vn (T.T. Ha), ducnb@daihoctantrao.edu.vn (N.B. Duc), hieuhk@duytan.edu.vn (H.K. Hieu).

https://doi.org/10.1016/j.radphyschem.2020.108979
Received 16 January 2020; Received in revised form 12 April 2020; Accepted 11 May 2020
Available online 04 July 2020

although phonon anharmonicity in cesium halides has been attracted attention of many authors, there is a lack of study considering the anharmonicity and thermal disorder in EXAFS. On the theoretical side, in order to analyze these effects in EXAFS for the first shell where the EXAFS analysis needs to consider only single scattering of the photoelectron emitted from the absorber as it hits upon one of its neighboring atoms, one usually applies a cumulant expansion approach in which an anharmonic EXAFS oscillation function χ(k) is expanded as follows (Bunker, 1983; Hung et al., 2011)

$$\chi(k) \sim Im\left\{e^{i\varphi(k)}\exp\left[2ikR + \sum_n \frac{(2ik)^n}{n!}C_n\right]\right\}, \tag{1}$$

where k the wave number, $\varphi(k)$ being net phase shift, r the instantaneous bond length between absorber and back-scatterer atoms, $R = \langle r \rangle$ denotes the thermal average distance, and $C_n (n = 1,2,3, ...)$ are the EXAFS cumulants. It should be noted that, beyond the first shell, the multiple scattering pathways between the back-scattering atom and the absorber atom need to be included. These multiple scattering contributions require a spherical wave correction. For Cu_2 system the order of the spherical part is about 5% of that of the plane wave part. And the spherical wave contribution at high temperature is larger than that of lower temperature. (Fujikawa et al., 1995)

In this paper, the thermal disorder and anharmonicity in cesium iodide are investigated in wide-range temperature based on an anharmonic correlated Debye model (Hung et al., 2010) (ACDM) in EXAFS theory. We organize this paper as follows in Section 2, the ACDM in EXAFS theory will be developed to derive the bond-streching force constants, the first three EXAFS cumulants and the anharmonic factor of B2-type CsI compound. Numerical calculations will be performed for CsI up to temperature 700 K using the Lennard-Jones potential combined with Coulomb interaction contribution in Section 3. Furthermore, in Section 3, the theoretical results are discussed in detail followed by Section 4 in which we make the conclusions of present work.

2. Theoretical approach

In this section, the ACDM (Hung et al., 2010; Duc et al., 2017; Hong et al., 2019) will be applied for CsI crystal with CsCl structure. The Debye model was proposed in condensed matter physics to estimate the phonon contribution to the specific heat of solid (Ashcroft and Mermin, 1976). This model assumes a homogeneous system having N oscillators propagated with a constant sound speed c, and vibrated with frequencies varied from 0 to the maximum phonon frequency ω_D, which is named the Debye frequency. The dispersion function in this model has a linear form $\omega = c.\ k$. The Debye temperature is defined as $\theta_D = \hbar\omega_D/k_B$ which can be seen as a criterion to classify the high and low temperature regions on the investigation of thermo-mechanical properties of material. In EXAFS theory, the correlated Debye model was proposed to determine the EXAFS Debye-Waller factor or parallel mean-square relative displacement (Rehr and Albers, 2000). The ACDM is a further development of the correlated Debye model which includes the contribution of anharmonicity to EXAFS cumulants through an anharmonic interatomic potential (Hung et al., 2010). This model considers a picture of local vibrations that takes into account correlations between absorber (A) and back-scatterer (B) atoms, and their nearest neighbors. It describes these interactions by the anharmonic interatomic effective potential V_{eff} which is characterized by a polynomial function of the thermal expansion $x = r - r_0$ as

$$\begin{aligned} V_{eff}(x) &= V(x) + \textstyle\sum_{j\neq i} V\left(\frac{\mu}{M_i}x.\ \hat{R}_{AB}.\ \hat{R}_{ij}\right) \\ &\approx \tfrac{1}{2}k_{eff}x^2 + k_3x^3 + ..., \qquad \mu = \tfrac{M_AM_B}{M_A+M_B}. \end{aligned} \tag{2}$$

In the above equation, r and r_0 being the instantaneous and equilibrium distances between absorber (with mass M_A) and back-scatterer (with mass M_B) atoms, respectively, and the term $V(x)$ characterizes the interaction potential between these two atoms. The second term in the right-hand side of Eq. (2) describes the influence of the nearest-neighbor atoms to the oscillations of absorber and back-scatterer, where the sum i is over absorber ($i = A$) and back-scatterer ($i = B$) atoms, and the sum j is over all their nearest neighbors, excluding the absorber and back-scatterer themselves. The parameter k_{eff} is the effective bond-stretching force constant, and k_3 is the cubic anharmonic parameter due to the asymmetry of the potential caused by an asymmetry in the pair distribution function.

In the following, the ACDM is applied for cesium iodide with CsCl structure (B2, $Pm\bar{3}m$). This structure of CsI is almost similar to body-centered cubic in which each corner is filled by an anion (or a cation), whereas the cation (or the anion) holds the center of the cell. In this structure, there are 14 pair interactions between absorber and back-scatterer atoms with their nearest neighbors, except for these two atoms themselves. The effective potential V_{eff} for CsI system then can be calculated as

$$\begin{aligned} V_{eff}(x) = V(x) + V(-\mu_A x) + 3V\left(-\tfrac{\mu_A x}{3}\right) + 3V\left(\tfrac{\mu_A x}{3}\right) \\ + V(-\mu_B x) + 3V\left(-\tfrac{\mu_B x}{3}\right) + 3V\left(\tfrac{\mu_B x}{3}\right), \end{aligned} \tag{3}$$

where non-dimensional parameters μ_A and μ_B are defined as

$$\mu_A = \frac{M_A}{M_A + M_B}, \quad \mu_B = \frac{M_B}{M_A + M_B}. \tag{4}$$

Assuming that the pair interaction between the ith and the jth particles in the CsI system can be described by the S-type "Coulomb-plus-Lennard-Jones" potential (Mile et al., 2012) which takes the following general form

$$V(r) = \frac{q_iq_j}{r} + \frac{A_iA_j}{r^{12}} - \frac{B_iB_j}{r^6}, \tag{5}$$

where q_i and q_j are charges on the interaction sites, whereas A_i, A_j, B_i and B_j are the Lennard-Jones parameterss.

By making the expansion of this "Coulomb-plus-Lennard-Jones" potential up to the third order of $x = r - r_0$, which is the deviation of instantaneous bond length r between two nearest-neighbor atoms from its equilibrium value r_0, we derive

$$V(x) \approx D_0 + D_1x + D_2x^2 + D_3x^3, \tag{6}$$

where

$$\begin{aligned} D_0 &= \tfrac{q_iq_j}{r_0} + \tfrac{A_iA_j}{r_0^{12}} - \tfrac{B_iB_j}{r_0^6}, \\ D_1 &= -\left(\tfrac{q_iq_j}{r_0^2} + 12\tfrac{A_iA_j}{r_0^{13}} - 6\tfrac{B_iB_j}{r_0^7}\right), \\ D_2 &= \tfrac{q_iq_j}{r_0^3} + 78\tfrac{A_iA_j}{r_0^{14}} - 21\tfrac{B_iB_j}{r_0^8}, \\ D_3 &= -\left(\tfrac{q_iq_j}{r_0^4} + 364\tfrac{A_iA_j}{r_0^{15}} - 56\tfrac{B_iB_j}{r_0^9}\right). \end{aligned} \tag{7}$$

Substituting Eq. (6) into Eq. (3) and comparing to Eq. (2) we obtain the force constants of CsI crystal in terms of Coulomb-plus-Lennard-Jones potential parameters as follows

$$\begin{aligned} k_{eff} &= 2D_2\left(1 + \tfrac{5}{3}\mu_A^2 + \tfrac{5}{3}\mu_B^2\right), \\ k_3 &= D_3(1 - \mu_A^3 - \mu_B^3). \end{aligned} \tag{8}$$

The Debye frequency ω_D and Debye temperature θ_D of the alloy system are calculated, respectively, as (Hung et al., 2010)

$$\omega_D = 2\sqrt{\frac{k_{eff}}{M}} \quad ; \quad \theta_D = \frac{\hbar\omega_D}{k_B}, \tag{9}$$

where M is a composite mass of alloy atoms.

In EXAFS theory, the thermal disorder can be described by means of the moments of atomic displacement so-called EXAFS cumulants. The second EXAFS cumulant is defined as the variance of the distance

distribution corresponding to the parallel mean-square relative displacement (Hieu and Hung, 2013; Ho et al., 2019). This parameter characterizes the EXAFS Debye-Waller factor of CsI. In the ACDM it was derived as (Hung et al., 2010)

$$C_2 = \langle x^2\rangle - \langle x\rangle^2 = -C_2^0 \int_0^{\pi/a} \omega(q)\frac{1+z(q)}{1-z(q)}dq, \tag{10}$$

where $C_2^0 = \frac{\hbar a}{2\pi k_{eff}}$ is the zero-point contribution to the second cumulant, $z(q) = \exp[\hbar\omega(q)/k_B T]$, k_B is the Boltzmann constant, T is the temperature in Kelvin, and the dispersion relation $\omega(q)$ is expressed as

$$\omega(q) = 2\sqrt{\frac{k_{eff}}{M}}\left|\sin\left(\frac{qa}{2}\right)\right|, \tag{11}$$

where a the lattice constant of system.

In order to consider anharmonic contributions to the second EXAFS cumulant, an anharmonic factor β was proposed with an argument analogous to the one (Willis and Pryor, 1975; Van Hung et al., 2003; Van Hung and Fornasini, 2007)

$$C_2^{total} = C_2 + \beta(C_2 - C_2^0),$$
$$\beta = 2\gamma_G\frac{\Delta V}{V}. \tag{12}$$

And we derive the analytical expression of the anharmonic factor as follows

$$\beta = 18\eta^2 C_2\left[1 - \frac{3\eta}{R}C_2\left(1 - \frac{\eta}{R}C_2\right)\right], \tag{13}$$

where $\eta = k_3/k_{eff}$.

As it can be seen from Eq. (13) that this factor is an increasing function of the second cumulant C_2 (and temperature) and inversely proportional to the shell radius. Then it reflects a similar property of anharmonicity obtained in an experimental catalysis research in which R is considered as atomic radius (Van Hung et al., 2003).

The third EXAFS cumulant characterizes the asymmetry of the pair distribution function affecting to the phase shift of EXAFS. It was calculated as

$$C_3 = \langle x^3\rangle - 3\langle x^2\rangle\langle x\rangle + 2\langle x\rangle^3$$
$$= C_3^0\int_0^{\pi/a} dq_1\int_{-\pi/a}^{\pi/a-q_1} F(q_1, q_2)dq_2, \tag{14}$$

where $C_3^0 = \frac{3\hbar^2a^2}{4\pi^2}\frac{k_3}{k_{eff}^3}$ is the zero-point contribution to the third EXAFS cumulant, and

$$F(q_1, q_2) = \frac{\omega(q_1)\omega(q_2)\omega(q_1+q_2)}{\omega(q_1)+\omega(q_2)+\omega(q_1+q_2)}\times$$
$$\times\left\{1 + 6\frac{\omega(q_1)+\omega(q_2)}{\omega(q_1)+\omega(q_2)-\omega(q_1+q_2)}\right.$$
$$\left.\frac{z(q_1)z(q_2)-z(q_1+q_2)}{[z(q_1)-1][z(q_2)-1][z(q_1+q_2)-1]}\right\}. \tag{15}$$

3. Numerical calculations and discussion

The expressions derived in the previous section are now applied to investigate the thermal disorder and anharmonicity of CsI system up to 700 K. At ambient pressure, the melting temperature of CsI is about 905 K (Haynes et al., 2017). The "Coulomb-plus-Lennard-Jones" potential parameters for CsI are shown in Table 1 (Aqvist, 1990; McDonald et al., 1998).

Using these potential parameters, we derive the effective spring constant $k_{eff} = 1.79$ eV/Å^2, correlated Debye frequency $\omega_D = 1.63\times10^{13}$ Hz and temperature $\theta_D = 124.76$ K, respectively. Our calculated Debye temperature $\theta_D = 124.76$ K for CsI agrees well with the Mössbauer scattering measurement of 125 K (Boyle and Perlow, 1966). Firstly, we consider the temperature dependence of the atomic mean-square

Table 1
The parameters of Coulomb-plus-Lennard-Jones potential for CsI (Aqvist, 1990; McDonald et al., 1998).

	$q_{i(j)}$ (e)	$A_{i(j)}$ (eV$^{1/2}$ Å^6)	$B_{i(j)}$ (eV$^{1/2}$ Å^3)
Cs	1.00	1647.90	5.44
I	−1.00	2734.05	17.36

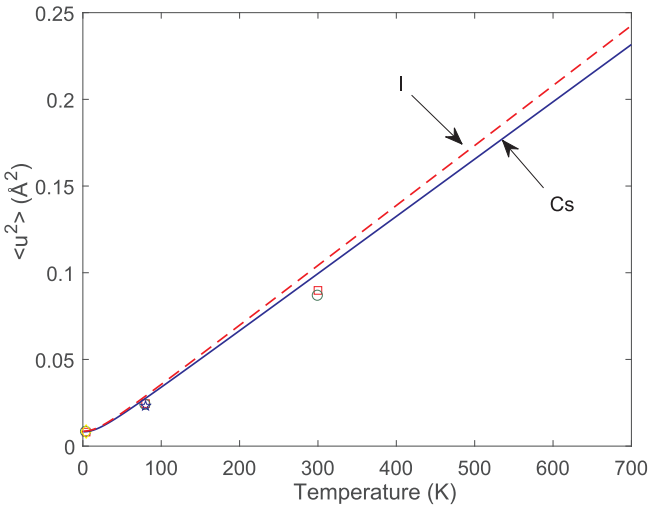

Fig. 1. Temperature dependence of atomic mean-square displacements in CsI. Previous measurements (Haridasan and Nandini, 1968; Boyle and Perlow, 1966) and calculated results of the deformation dipole model (Agrawal et al., 1975) are also shown for comparison.

displacement. In Debye model, this quantity can be calculated by the following expression (Skelton and Katz, 1968)

$$\langle u^2\rangle = \frac{9\hbar^2}{mk_B\theta_M}\left[\frac{\Phi(\theta_M/T)}{\theta_M/T} + \frac{1}{4}\right], \tag{16}$$

where $\Phi(\theta_M/T)$ being the Debye function, and θ_M is a characteristic temperature which would be the Debye temperature for a Debye solid. In the work of Boyle and Perlow (1966), the authors pointed out a relation $\theta_D = 1.25\theta_M$ for CsI. From this, we derive $\theta_M = 99.81$ K. In Fig. 1, we show the mean-square displacements of Cs and I as functions of temperature. Previous measurements (Haridasan and Nandini, 1968; Boyle and Perlow, 1966) and calculated results of the deformation dipole model (DDM) (Agrawal et al., 1975) have also been showed for comparison. Values of the mean-square displacements of Cs and I at temperature 4, 80 and 300 K are presented in Table 2. At low temperatures ($T < 100$ K), the good agreement between our results and previous works is found. The difference between the Debye model and DDM tends to increase with increasing temperature. This disagreement between two methods may be because the characteristic temperature θ_M is assumed to be independent to temperature, and the Debye-Waller factors are isotropic under the harmonic approximation of the Debye model.

In the following, the derived force constants k_{eff} and k_3, and the correlated Debye frequency ω_D are used to consider the temperature effects on the EXAFS thermodynamic quantities. In Fig. 2 we show the temperature dependence of the Debye-Waller factor which corresponds to the parallel atomic mean-square relative displacement of CsI system up to 700 K. As observed in this figure, the second EXAFS cumulant C_2 rapidly increases with temperature, and beyond 50 K, it is almost linear proportional to temperature. The mean slope of the cumulant C_2 in temperature range 50 K–700 K is approximately $dC_2/dT = 4.73\times10^{-5}$ Å^2/K. The rough increase of the Debye-Waller factor means that the thermal disorder gives an important contribution at high temperature.

Table 2
Atomic mean-square displacements in CsI (Gerlich and Andersson, 1982).

Temperature (K)	Present calculations		DDM (Agrawal et al., 1975)		Expt. (Haridasan and Nandini, 1968)		Expt. (Boyle and Perlow, 1966)	
	$\langle u^2\rangle_{Cs}$	$\langle u^2\rangle_I$	$\langle u^2\rangle_{Cs}$	$\langle u^2\rangle_I$	$\langle u^2\rangle_{Cs}$	$\langle u^2\rangle_I$	$\langle u^2\rangle_{Cs}$	$\langle u^2\rangle_I$
4	0.00834	0.00873	0.00809	0.00813	0.0084	–	0.0083	–
80	0.02758	0.02889	0.02453	0.02377	–	0.0232	–	–
300	0.09951	0.10422	0.08979	0.08666	–	–	–	–

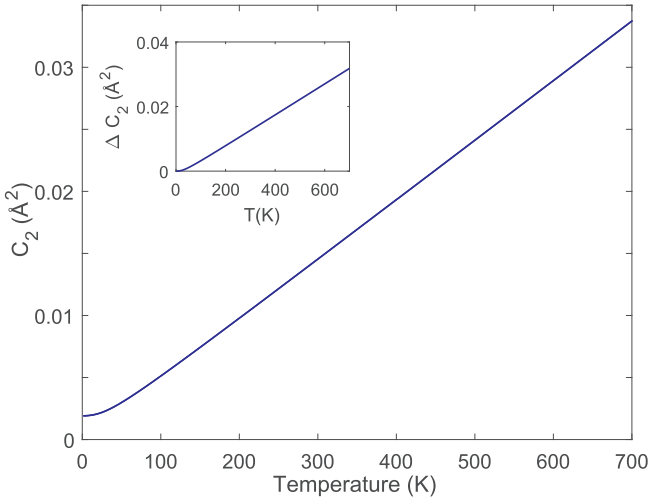

Fig. 2. Temperature dependence of the second cumulant of CsI.

Here it is worth mentioning that the second cumulant C_2 influences on the amplitude of EXAFS oscillations through the factor $W(k) = \exp(-2C_2k^2)$. (Crozier et al., 1988) The robust increasing of C_2 will make a large reduction in the amplitude of EXAFS spectra.

In order to get a clear picture of the contributions of anharmonicity to C_2, we show the anharmonic factor β of CsI as a function of temperature in Fig. 3. The calculated anharmonic factor of Cu has also been displayed for comparison. As it can be observed from this figure, the anharmonic factor of CsI is essentially higher than that of the reference one (Cu). Substituting the calculated β into Eq. (12), we derive the total second EXAFS cumulant which is plotted in Fig. 4. This result shows that below 20 K the anharmonic contribution to C_2 of CsI is small but different from zero. This behavior of CsI departs from Cu metal, where the anharmonic contribution was unveiled almost zero at temperature

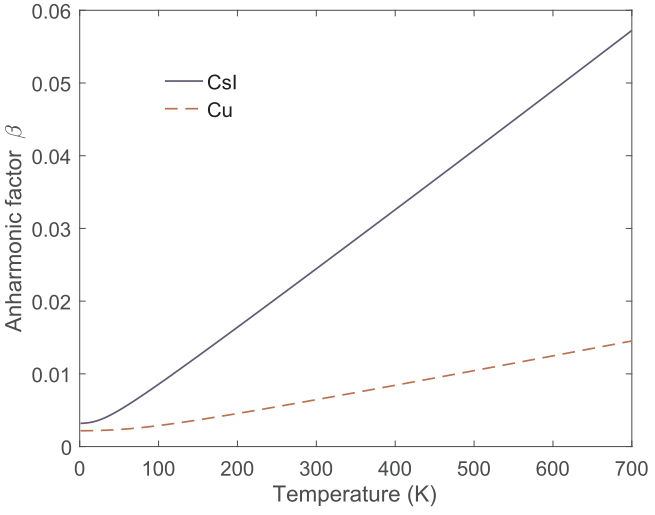

Fig. 3. Temperature dependence of the anharmonic factor of CsI.

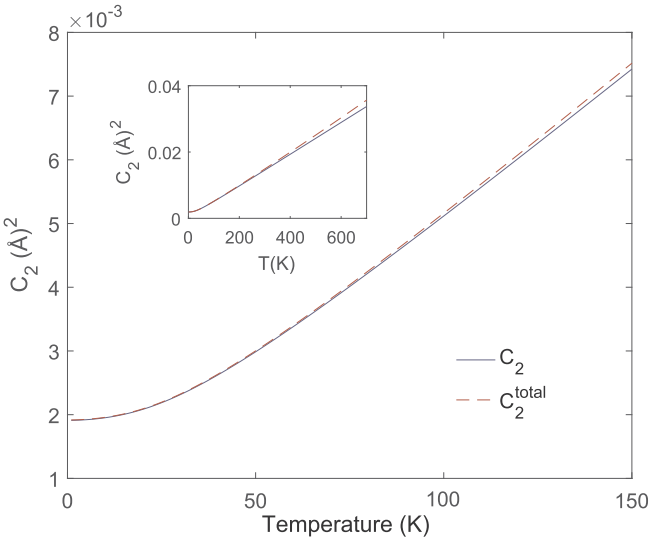

Fig. 4. Temperature dependence of the total second cumulant of CsI.

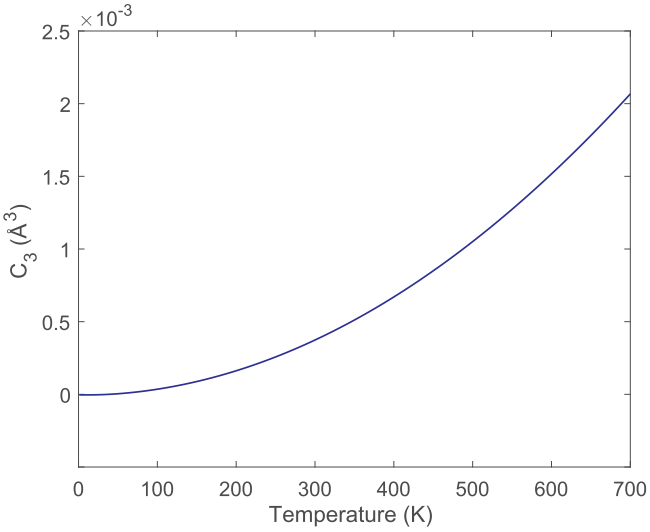

Fig. 5. Temperature dependence of the third cumulant C_3 of CsI.

below 100 K (Van Hung et al., 2003).

In Fig. 5, we present the anharmonic parameter C_3 as a function of temperature obtained from the ACDM up to 700 K. As it can be seen from this figure, there is non linear increase of the third cumulant C_3 with increasing temperature. The increase of asymmetric parameter C_3 causes the deviation of the effective distribution function from a harmonic Gaussian approximation. The third cumulant curve in our calculations is well fitted by a quadratic function of temperature as $C_3(T) = a_0 + a_1T + a_2T^2$, with $a_0 = -6.12 \times 10^{-6}$ Å^3, $a_1 = -4.24 \times 10^{-9}$ Å^3/K, and $a_2 = 4.24 \times 10^{-9}$ Å^3/K^2.

Now we consider the temperature dependence of a cumulant ratio C_r which is defined through EXAFS cumulants as $C_r = C_1.\ C_2/C_3$ (Hung

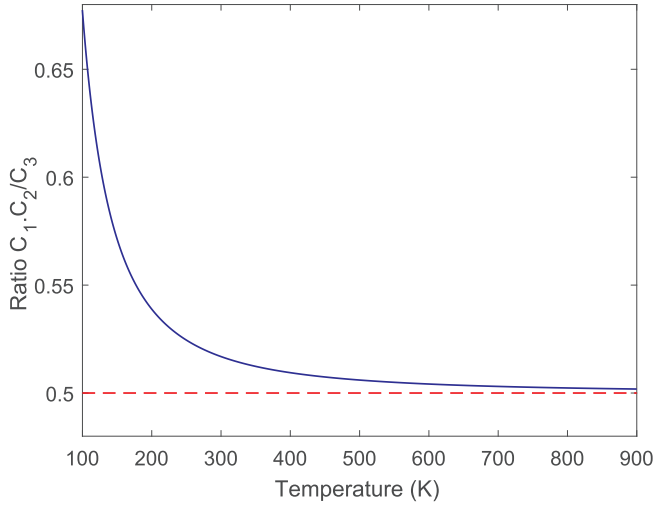

Fig. 6. Temperature dependence of the cumulant ratio C_r of CsI.

and Rehr, 1997). Previous researches showed that this ratio can be seen as a criterion for cumulant investigation. At high temperature limit, the cumulant ratio C_r tends to a constant value of $1/2$, and the ratio can be applied to derive the temperature threshold of classical limit region. In Fig. 6, we show the temperature-dependent cumulant ratio C_r of CsI calculated within the present ACDM approach. As observed from this figure, the cumulant ratio drops rapidly at temperature $T \geq 300$ K. Beyond 300 K, the cumulant ratio depresses gradually, and tends to $1/2$ at $T \geq 700$ K. Then we deduce that the threshold temperature at which the classical calculations can be applicable, is about 700 K.

Before making conclusions, it should be noted that although the cumulant expansion technique is a simple method to investigate the anharmonicity and thermal disorder in EXAFS, it does not provide a reliable reconstruction of the distance distribution function. This comes from a truth that adding only the third cumulant is not enough to define the distribution itself. Furthermore, in most of previous works, the ACDM was applied to determine the temperature-dependent EXAFS cumulants of monoatomic crystals such as Cu, Ni metals. In this work, the ACDM has been developed for CsI compound considering not only pair interaction potentials but also Coulomb interaction potentials between charges. The present approach can be easily applied for other binary compounds with CsCl structure to consider EXAFS cumulants, anharmonicity as well as thermal disorder. Moreover, the temperature dependence of EXAFS cumulants can be studied by means of various techniques such as Debye model (Hung et al., 2010; Duc et al., 2017; Hong et al., 2019), path-integral effective-potential (PIEP) approach (Yokoyama, 1998; Miyanaga and Fujikawa, 1998) or computer simulation including density functional theory (DFT) calculations. However, the estimation of odd-order anharmonicity at low temperature in the PIEP method is not good. For example, in the calculation of C_3 in Br_2, it shows a strange decrease at the temperature less than 100 K. This phenomenon can be explained that vibrational properties tends to be harmonic at 0 K limit in the PIEP approach (Yokoyama, 1998). Meanwhile the advantage of ACDM in comparison with DFT calculations is the apparent analytical expressions of EXAFS cumulants, the Debye-Waller factor and anharmonic factor. These formulae allow us easily and quickly determine the EXAFS parameters of systems at various temperature.

4. Conclusions

In this work, the thermal disorder and anharmonicity of cesium iodide have been investigated by using the anharmonic correlated Debye model in EXAFS theory. Numerical calculations of the EXAFS Debye-Waller factor, the anharmonic factor and the third cumulant of CsI have been performed up to temperature 700 K using the Lennard-Jones potential combined with Coulomb interaction contribution. Our research showed that the anharmonicity of thermal lattice vibrations gave important contributions to the EXAFS cumulants. By investigation of the anharmonic factor we highlight the importance of anharmonicity not only at high temperature but also at low temperature in CsI crystal. This behavior of CsI departs from Cu transition metal, where the anharmonic contribution was unveiled almost zero at temperature below 100 K.

CRediT authorship contribution statement

Tran Thi Ha: Data curation, Formal analysis, Investigation, Methodology, Writing - original draft, Writing - review & editing. **Nguyen Ba Duc:** Resources, Project administration, Funding acquisition, Supervision, Investigation, Writing - original draft, Writing - review & editing. **Nguyen Van Nghia:** Validation, Writing - review & editing. **Pham Thi Minh Hanh:** Validation, Visualization, Writing - review & editing. **Vu Thi Thanh Ha:** Validation, Visualization, Writing - review & editing. **Ho Khac Hieu:** Conceptualization, Resources, Validation, Writing - original draft, Writing - review & editing.

Declaration of competing interest

The authors declare that they have no known competing financial interests or personal relationships that could have appeared to influence the work reported in this paper.

Acknowledgements

The authors would like to acknowledge Prof. Nguyen Van Hung and two anonymous reviewers for their useful comments and suggestions. This research is funded by the Vietnam National Foundation for Science and Technology Development (NAFOSTED) under grant number 103.01–2019.55.

Appendix A. Supplementary data

Supplementary data to this article can be found online at https://doi.org/10.1016/j.radphyschem.2020.108979.

References

Agrawal, B.S., Beaver, J.P., Weymouth, J.W., Hardy, J.R., 1975. Acta Crystallogr. A 31, 249. https://doi.org/10.1107/S0567739475000502.
Aqvist, J., 1990. J. Phys. Chem. 94, 8021. https://doi.org/10.1021/j100384a009. eprint.
Ashcroft, N.W., Mermin, N.D., 1976. Solid State Physics, first ed. Cengage Learning. https://www.amazon.com/Solid-State-Physics-Neil-Ashcroft/dp/0030839939.
Bang, Y., Choi, H.-Y., Won, H., 2009. Phys. Rev. B 79, 54529. https://link.aps.org/doi/10.1103/PhysRevB.79.054529.
Bansal, D., Niedziela, J.L., Sinclair, R., Garlea, V.O., Abernathy, D.L., Chi, S., Ren, Y., Zhou, H., Delaire, O., 2018. Nat. Commun. 9, 15. https://doi.org/10.1038/s41467-017-02309-2. 2041–1723.
Bingol, Suat, Erdinc, Bahattin, Akkus, Harun, 2015. Int. J. Simul. Multidiscip. Des. Optim. 6, A7. https://doi.org/10.1051/smdo/2015007.
Boyle, A.J.F., Perlow, G.J., 1966. Phys. Rev. 151, 211. https://link.aps.org/doi/10.1103/PhysRev.151.211.
Bunker, G., 1983. Nucl. Instrum. Methods Phys. Res. 207, 437. http://www.sciencedirect.com/science/article/pii/0167508783906555 0167–5087.
Cicco, A.D., Rosolen, M.J., Marassi, R., Tossici, R., Filipponi, A., Rybicki, J., 1996. J. Phys. Condens. Matter 8, 10779. https://doi.org/10.1088/0953-8984/8/50/007.
Di Cicco, A., Taglienti, M., Minicucci, M., Filipponi, A., 2000. Phys. Rev. B 62, 12001. https://link.aps.org/doi/10.1103/PhysRevB.62.12001.
Crozier, E.D., Rehr, J.J., Ingalls, R., 1988. X-Ray Absorption: Principles, Applications, Techniques of EXAFS, SEXAFS and XANES. In: Koningsberger, D.C., Prins, R. (Eds.), first ed. Wiley-Interscience0471875473, . http://www.amazon.com/X-Ray-Absorption-Principles-Applications-Techniques/dp/0471875473.
Duc, N.B., Tho, V.Q., Hung, N.V., Khoa, D.Q., Hieu, H.K., 2017. Vacuum 145, 272. 0042–207X. http://www.sciencedirect.com/science/article/pii/S0042207X17307716.
Fujikawa, T., Yimagawa, M., Miyanaga, T., 1995. Phys. B Condens. Matter 208–209, 91. proceedings of the 8th International Conference on X-ray Absorption Fine Structure,

0921–4526. http://www.sciencedirect.com/science/article/pii/0921452694006418.
Gerlich, D., Andersson, P., 1982. J. Phys. C Solid State Phys. 15, 5211. https://doi.org/10.1090/s0002-9939-2011-10822-0.
Haridasan, T., Nandini, R., 1968. Phys. Lett. 28, 301. 0375–9601. http://www.sciencedirect.com/science/article/pii/0375960168902971.
Haynes, W., Lide, D., Bruno, T., 2017. CRC Handbook of Chemistry and Physics, 97th ed. CRC Press.
Van Hung, N., Fornasini, P., 2007. J. Phys. Soc. Jpn. 76, 84601. https://doi.org/10.1143/JPSJ.76.084601.
Hieu, H.K., Hung, V.V, 2013. High Pressure Res. 33 (4), 768–776. https://doi.org/10.1080/08957959.2013.849346.
Ho, H.K., Nguyen, V.T., Nghia, N.V., Duc, N.B., Tho, V.Q., Hai, T.T., Khoa, D.Q., 2019. Curr. Appl. Phys. 19 (1), 55–59. https://doi.org/10.1016/j.cap.2018.11.005.
Hong, N.T., Hieu, H.K., Duc, N.B, Phuong, D.D., Tuyen, N.V., Khoa, D.Q., 2019. Vacuum 163, 210–215. https://doi.org/10.1016/j.vacuum.2019.02.023.
Hung, V.V, Hieu, H.K., Masuda-Jindo, K., 2010. Comput. Mater. Sci. 49 (4), S214–S217. https://doi.org/10.1016/j.commatsci.2010.02.005.
Hung, N.V., Hung, V.V, Hieu, H.K., Frahm, R.R, 2011. Physica B: Condens. Matter 406 (3), 456–460. https://doi.org/10.1016/j.physb.2010.11.012.
Hung, N.V., Rehr, J.J., 1997. Phys. Rev. B 56, 43. http://link.aps.org/doi/10.1103/PhysRevB.56.43.
Van Hung, N., Ba Duc, N., Frahm, R.R., 2003. J. Phys. Soc. Jpn. 72, 1254. https://doi.org/10.1143/JPSJ.72.1254.
Hung, N.V., Trung, N.B., Kirchner, B., 2010. Phys. B Condens. Matter 405, 2519. 0921–4526. http://www.sciencedirect.com/science/article/pii/S0921452610002656.
Li, C.W., Tang, X., Muñoz, J.A., Keith, J.B., Tracy, S.J., Abernathy, D.L., Fultz, B., 2011. Phys. Rev. Lett. 107, 195504. https://link.aps.org/doi/10.1103/PhysRevLett.107.195504.
Li, C.W., Hong, J., May, A.F., Bansal, D., Chi, S., Hong, T., Ehlers, G., Delaire, O., 2015. Nat. Phys. 11, 1063. https://doi.org/10.1038/nphys3492.
McDonald, N.A., Duffy, E.M., Jorgensen, W.L., 1998. J. Am. Chem. Soc. 120, 5104. https://doi.org/10.1021/ja980140x.
Mile, V., Gereben, O., Kohara, S., Pusztai, L., 2012. J. Phys. Chem. B 116, 9758. https://doi.org/10.1021/jp301595m. pMID: 22794148.
Miyanaga, T., Fujikawa, T., 1998. J. Phys. Soc. Jpn. 67, 2930. https://doi.org/10.1143/JPSJ.67.2930.
Rehr, J.J., Albers, R.C., 2000. Rev. Mod. Phys. 72, 621. http://link.aps.org/doi/10.1103/RevModPhys.72.621.
Sist, M., Fischer, K.F.F., Kasai, H., Iversen, B.B., 2017. Angew. Chem. Int. Ed. 56, 3625. eprint. https://onlinelibrary.wiley.com/doi/pdf/10.1002/anie.201700638. https://onlinelibrary.wiley.com/doi/abs/10.1002/anie.201700638.
Skelton, E.F., Katz, J.L., 1968. Phys. Rev. 171, 801. https://link.aps.org/doi/10.1103/PhysRev.171.801.
Wei, B., Yu, X., Yang, C., Rao, X., Wang, X., Chi, S., Sun, X., Hong, J., 2019. Phys. Rev. B 99, 184301. https://link.aps.org/doi/10.1103/PhysRevB.99.184301.
Willis, T.M., Pryor, A.W., 1975. Thermal Vibrations in Crystallography. Cambridge University Press, Cambridge, U.K.
Yokoyama, T., 1998. Phys. Rev. B 57, 3423. http://link.aps.org/doi/10.1103/PhysRevB.57.3423.